Signal Processing Seminar
Developing Good Practice in Metrology Applications
30th November 2005 - NPL, Teddington, UK

Algorithms, Applications and Systems for Digital Signal Processing

Patrick Gaydecki

School of Electrical and Electronic Engineering
The University of Manchester
PO Box 88
Manchester M60 1QD
United Kingdom

www.sisp.manchester.ac.uk/dsp.shtml
patrick.gaydecki@manchester.ac.uk
[UK-44] (0) 161 306 4906

Overview of Presentation

- The advantages of real-time DSP in weak signal detection
- Typical real-time DSP hardware and software specifications
- Finite impulse response (FIR) design and applications
- Infinite Impulse response design and applications
- Inverse filter design and applications
- Case study: weak AC magnetic field detection

Characteristics of Real-Time DSP Systems

- DSP offers flexibility, allowing a single platform to be rapidly reconfigured for different applications
- Operations such as modulation, phase shifting, signal mixing and delaying are simply performed in software
- System performance is far more accurate than equivalent analogue systems
- However, considerable intellectual investment is required to design and program DSP platforms

DSP Hardware and Software Specifications (Signal Wizard, Developed at UoM)

- 24-bit codec resolution (1 part in 16777216, or 144 dB)
- Variable sample rate extending to 196 kHz
- Processor power of 100 million multiplication-accumulations per second (MMACS)
- Dual channel operation for signal referencing and mixing
- Non-volatile memory for retention of settings
- Standard PC interface
- Easy FIR, and IIR filter design, with other processing functions including mixing and phasing

Anatomy of a Typical DSP Device

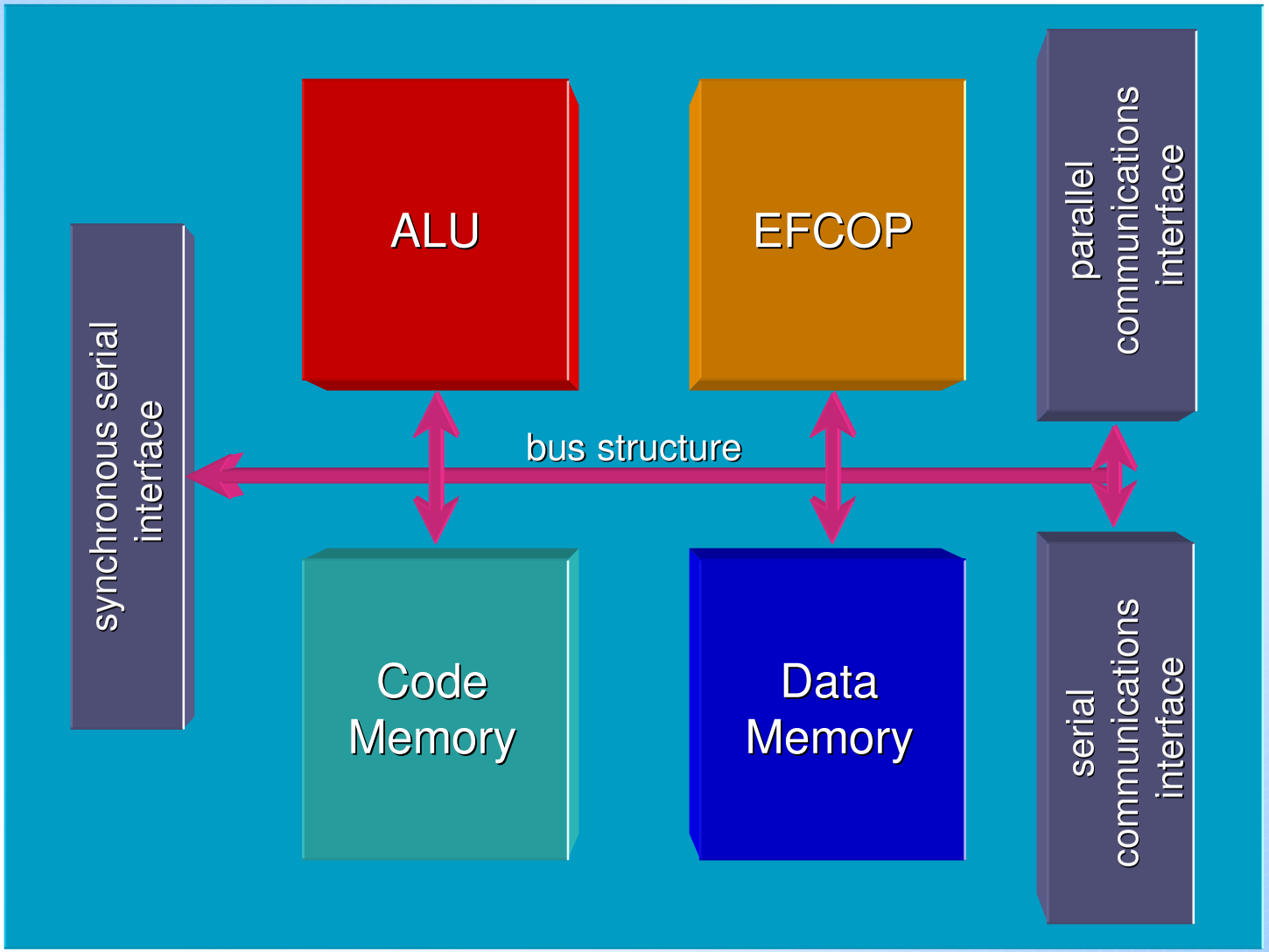

Components of the Real-Time DSP System

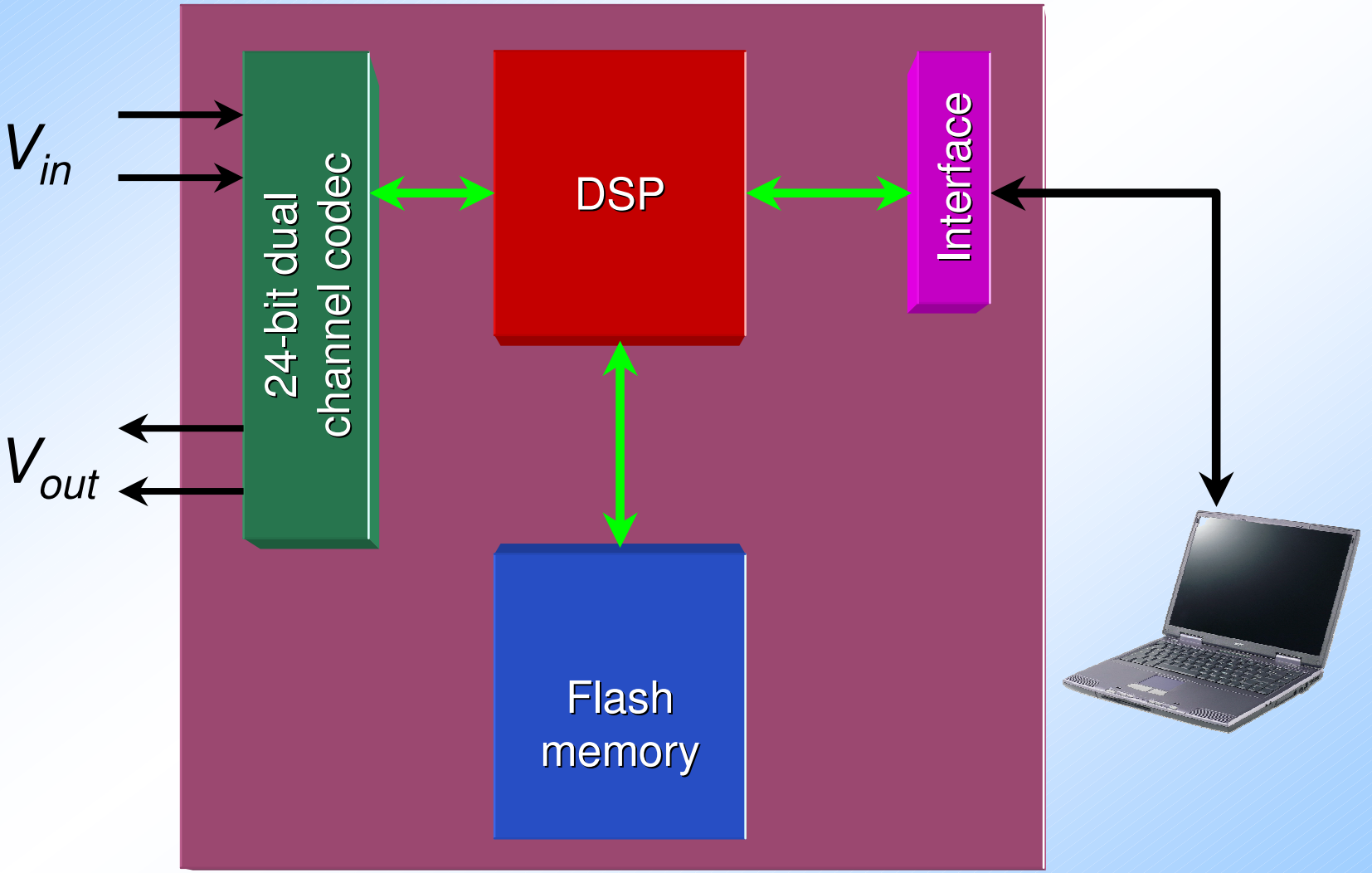

The Inherent Versatility of the Synchronous Serial Interface

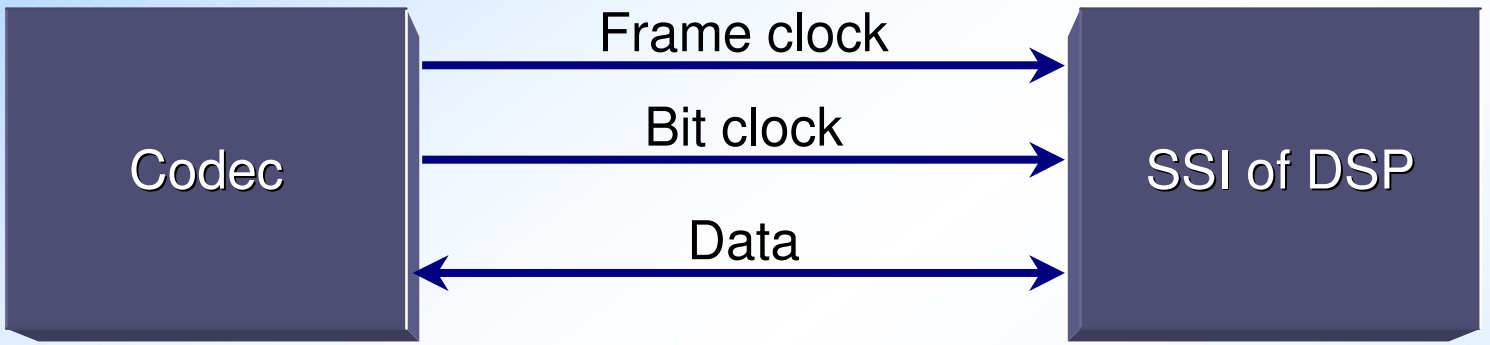

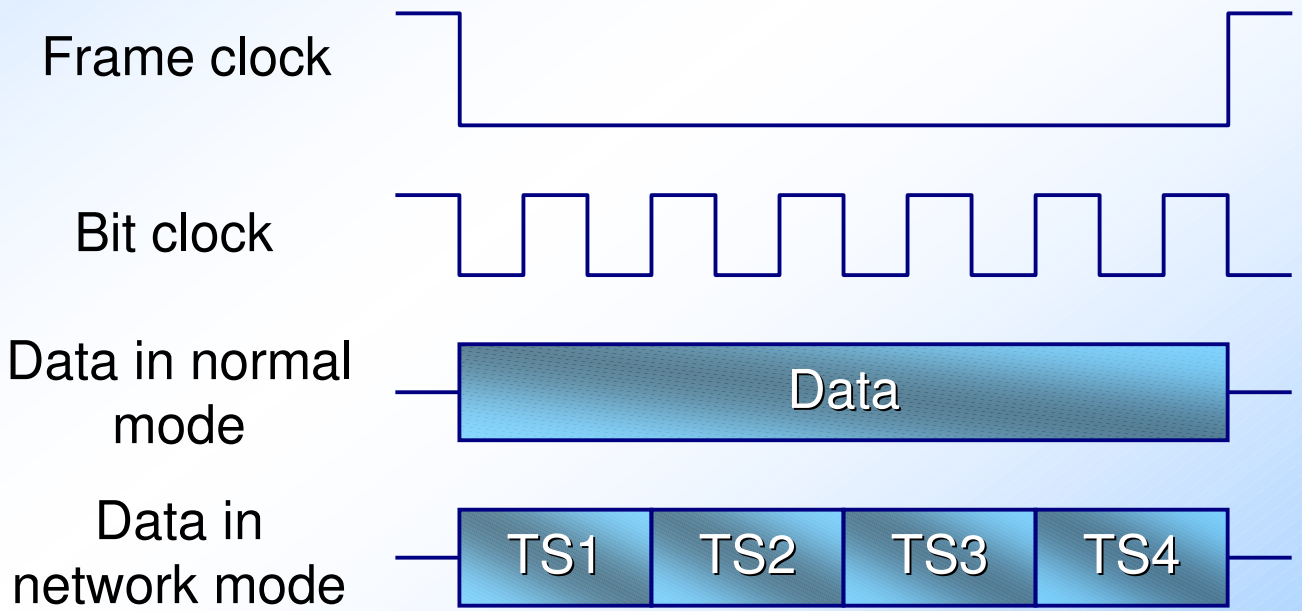

FIR Performance Figures for DSP56309 and DSP56321

Sample frequency, kHz	Nyquist frequency, kHz	Filter coefficients, DSP56309	Filter coefficients, DSP56321
10	5	9888	55000
20	10	4888	27500
40	20	2489	13750
100	50	888	5500
200	100	450	2750
500	250	195	1100
1000	500	85	550

Final Realized Hardware (Signal Wizard)

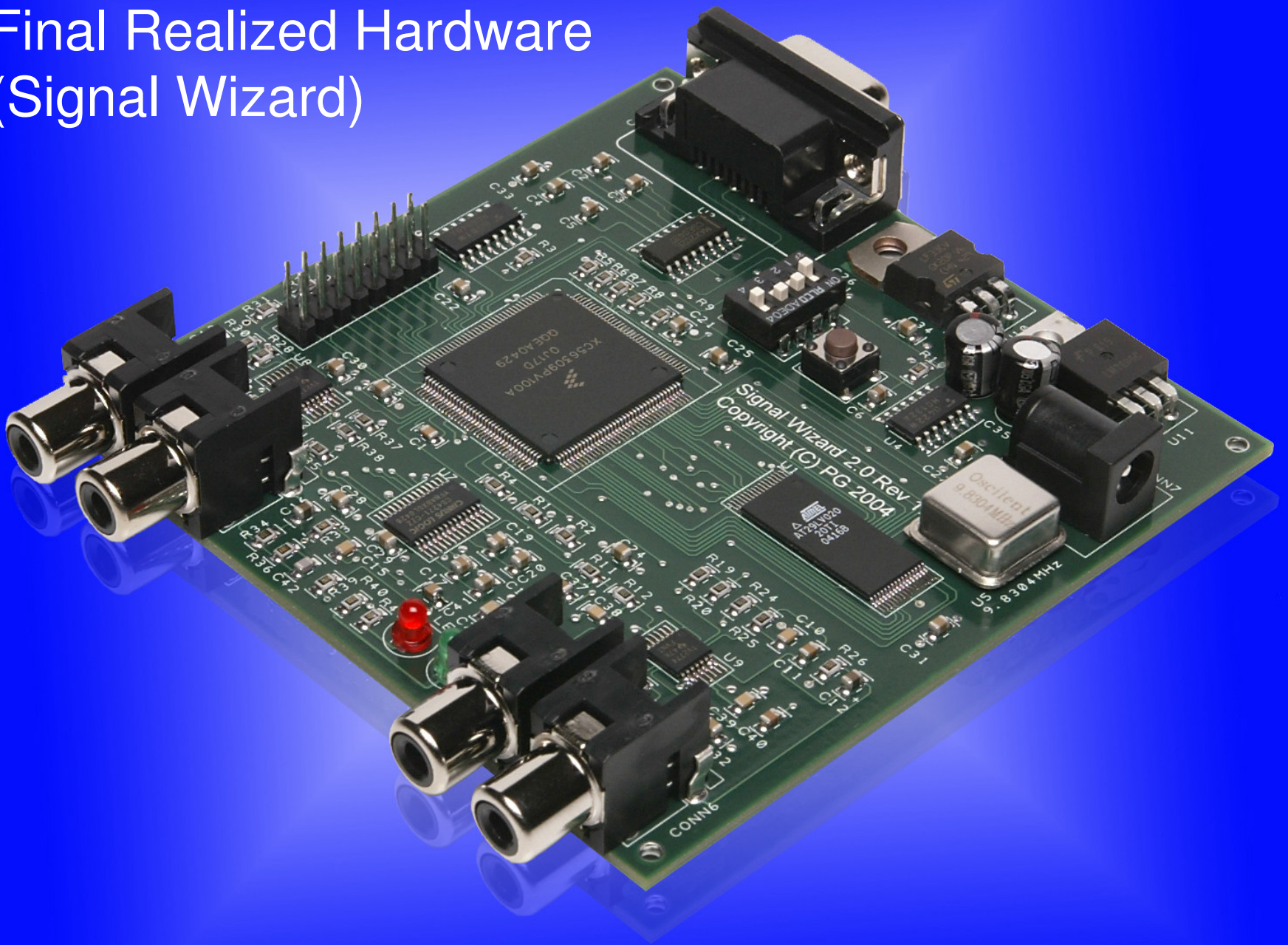

Final Realized Software (Signal Wizard)

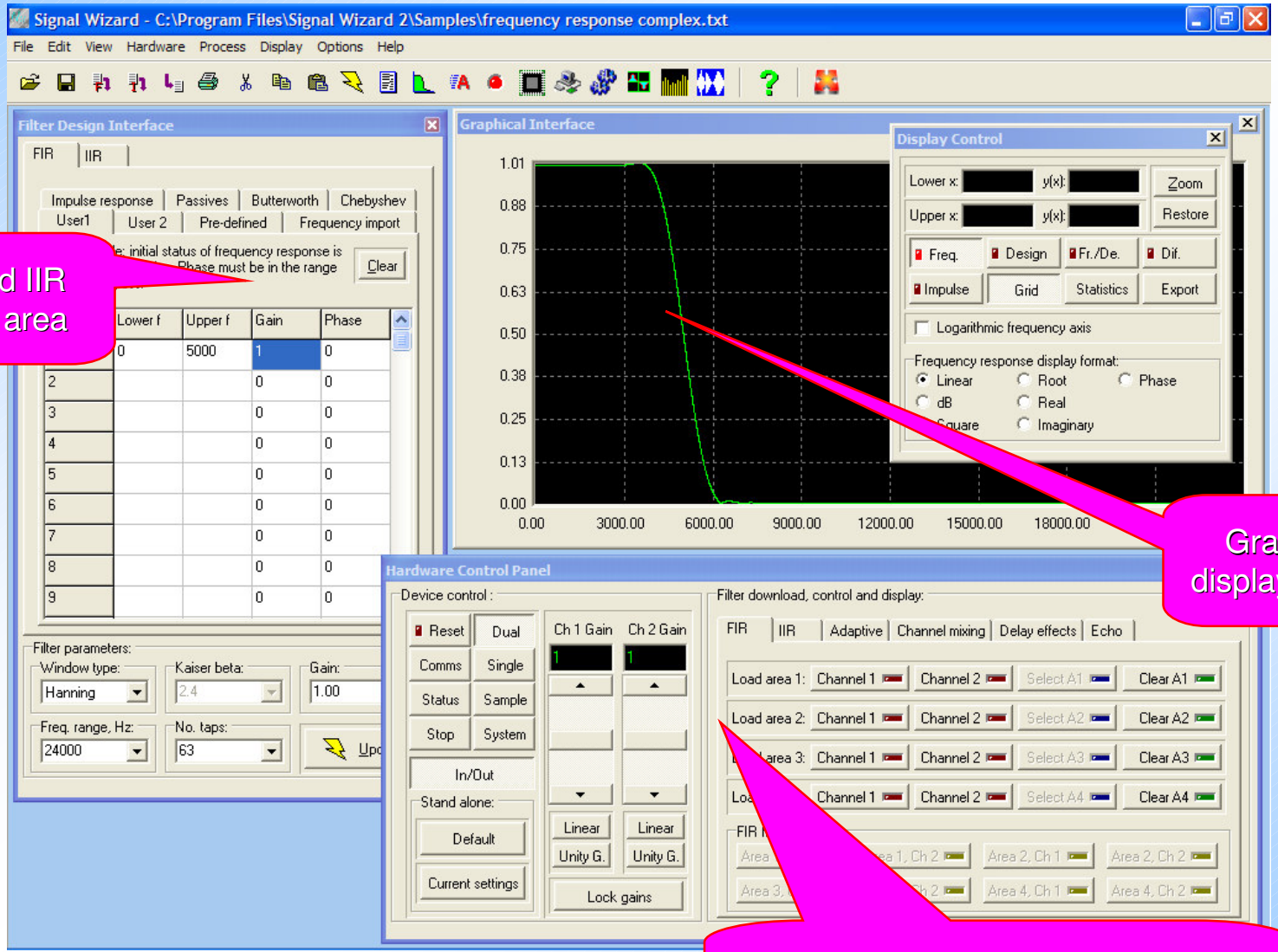

FIR and IIR design area

Graphical display of filter

Hardware control: download, gain, adaptive, delay, mixing etc.

Basic Linear Filter Theory: $y(t) = \int_{-\infty}^{\infty} h(\tau)x(t-\tau)d\tau$

Property / Filter type	FIR	IIR
Output signal	$y[n] = \sum_{k=0}^{M-1} h[k]x[n-k]$	$y[n] = \sum_{k=0}^{N} a[k]x[n-k] - \sum_{k=1}^{M} b[k]y[n-k]$
Transfer function	$H(z) = \frac{Y(z)}{X(z)} = \sum_{n=0}^{\infty} h[n]z^{-n}$	$H(z) = \frac{a[0]+a[1]z^{-1}+\ldots+a[m]z^{-m}}{1+b[1]z^{-1}+\ldots+b[n]z^{-n}} = \frac{\sum_{m=0}^{M} a[m]z^{-m}}{1+\sum_{n=1}^{N} b[n]z^{-n}}$
Unconditional stability	yes	no
Word length immunity	good	poor
Design ease	easy	unwieldy
Arbitrary response	yes	not in practice
Computational load	high	low
Analogue equivalent	yes	yes

Finite Impulse Response (FIR) Filter Design using the Frequency Sampling Approach

Arbitrary filter impulse response $h[n]$ obtained by:

$$h[n] = w[n]F^{-1}\left[H[k]\right] \qquad \begin{cases} H_r[k] = a[k] & f_l < k < f \\ H_i[k] = b[k] & f_l < k < f \\ H_r[k] = 0 & \text{elsewhere} \\ H_i[k] = 0 & \text{elsewhere} \end{cases}$$

Output signal $y[n]$ obtained by discrete-time convolution:

$$y[n] = \sum_{k=0}^{M-1} h[k]x[n-k]$$

Windowing: Blackman v Rectangular

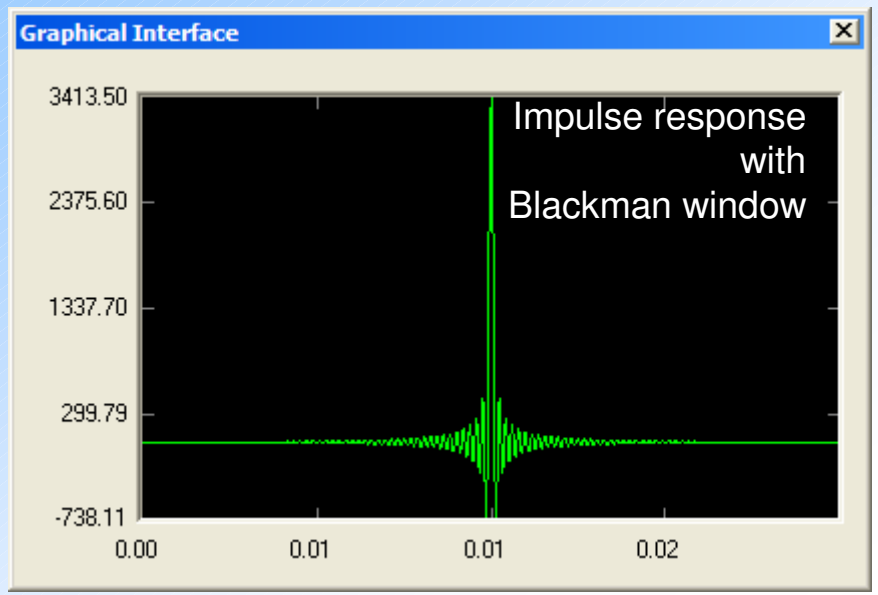

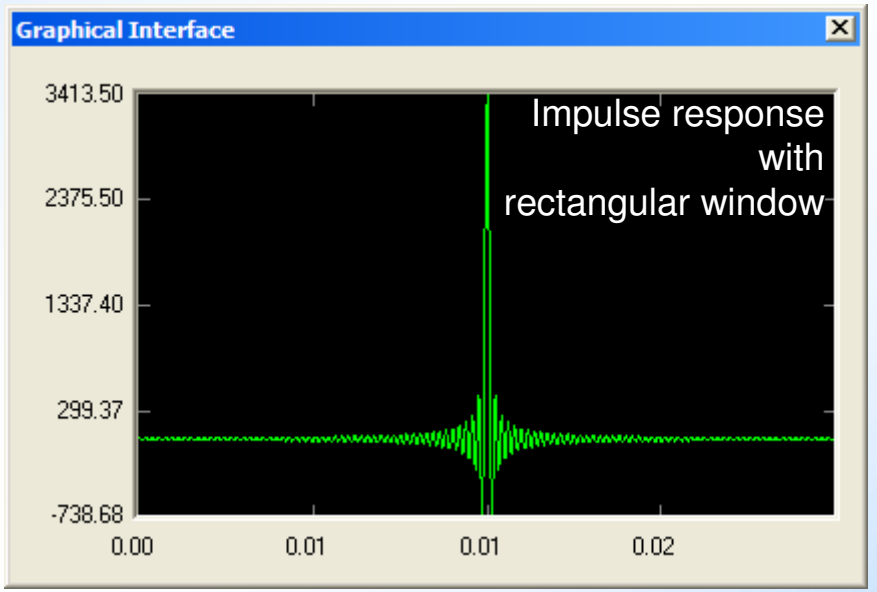

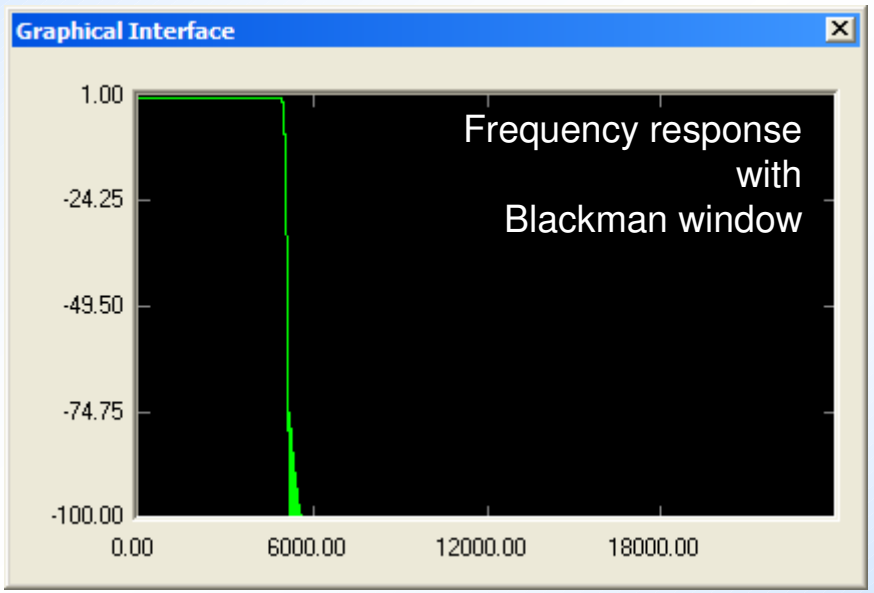

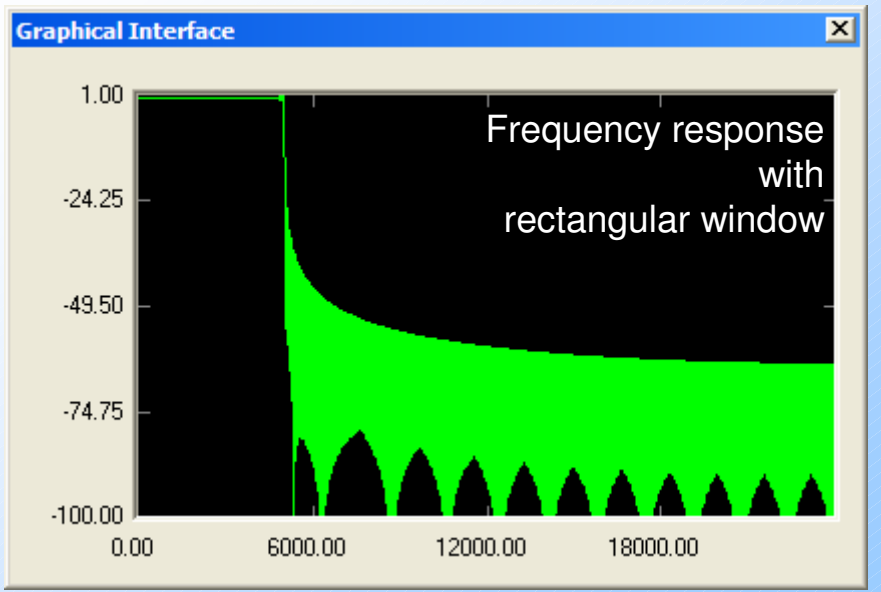

Phase Control

Precise phase control for each harmonic, to a resolution of 0.0001 degree. Application: real-time Hilbert transform.

$$Y_h(\omega) = \begin{cases} -jY(\omega), & \omega > 0 \\ jY(\omega), & \omega < 0 \end{cases}$$

$$y_h(t) = H\{y(t)\} = F^{-1}\{Y_h(\omega)\}$$

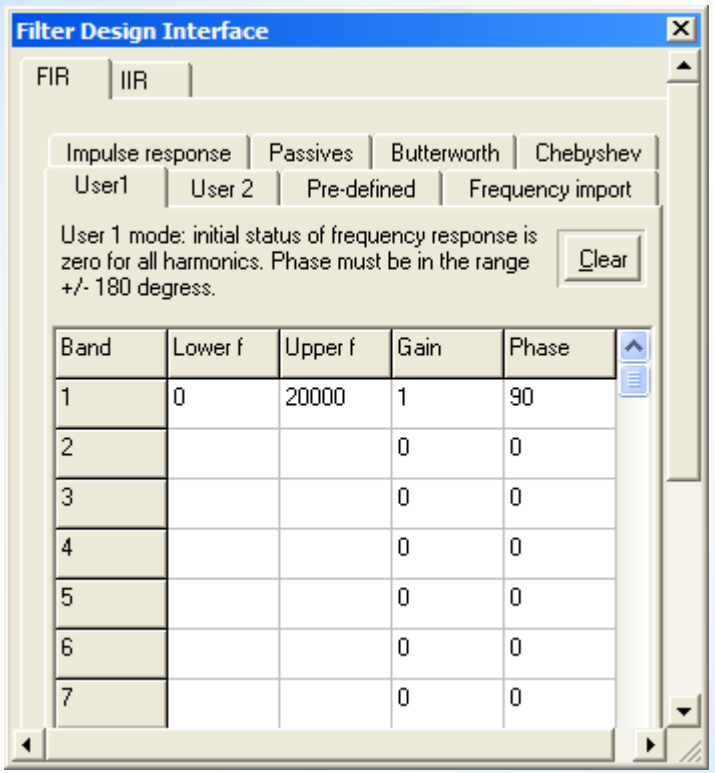

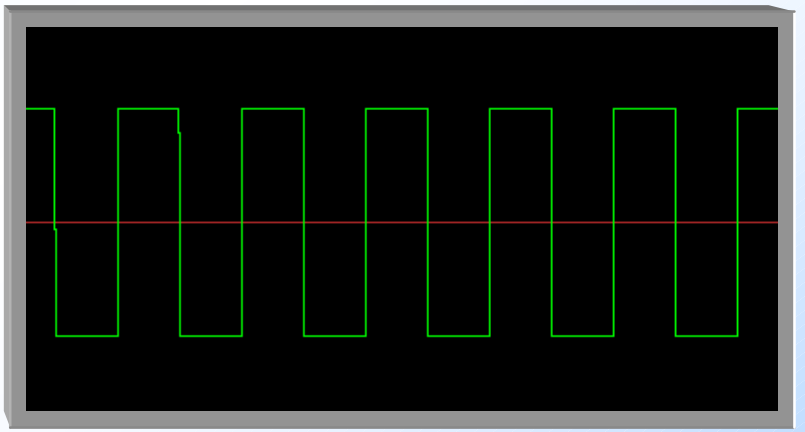

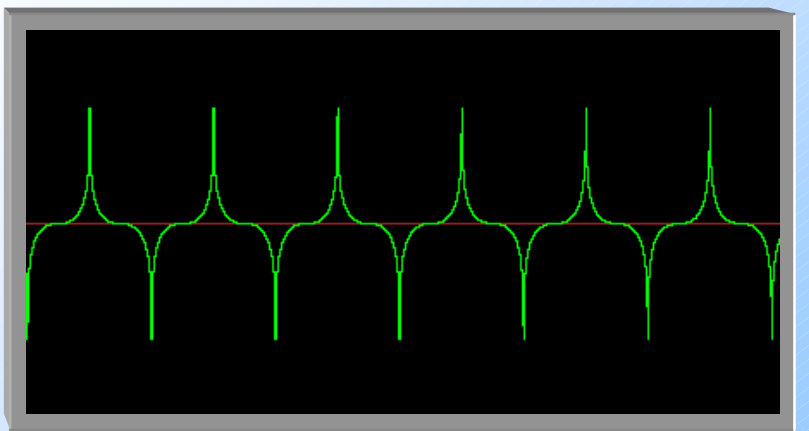

Infinite Impulse Response (IIR) Filter Design

$$y[n] = \sum_{k=0}^{N} a[k]x[n-k] - \sum_{k=1}^{M} b[k]y[n-k]$$

Digital Emulation of Analogue Networks I: Laplace to z-domain mapping

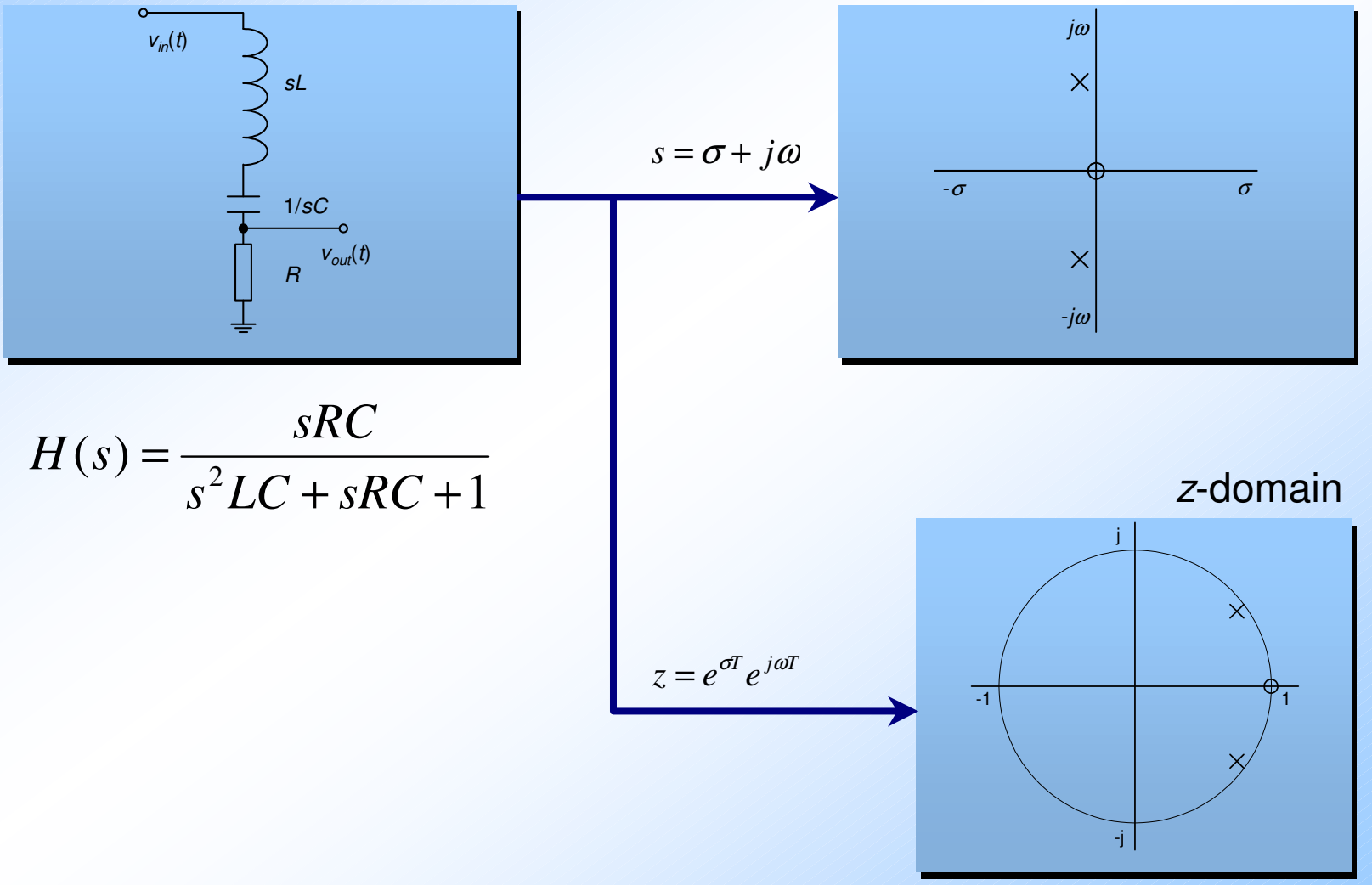

Digital Emulation of Analogue Networks II: The Bilinear z-transform (BZT)

$$H(s) = \frac{sRC}{s^2LC + sRC + 1}$$

$$H(z) = \frac{\frac{2}{T}RC\left[\frac{1-z^{-1}}{1+z^{-1}}\right]}{\left(\frac{2}{T}\right)^2 LC\left[\frac{1-z^{-1}}{1+z^{-1}}\right]^2 + \frac{2}{T}RC\left[\frac{1-z^{-1}}{1+z^{-1}}\right] + 1}$$

$$H(z) = \frac{a\left[\frac{1-z^{-1}}{1+z^{-1}}\right]}{b\left[\frac{1-z^{-1}}{1+z^{-1}}\right]\left[\frac{1-z^{-1}}{1+z^{-1}}\right] + a\left[\frac{1-z^{-1}}{1+z^{-1}}\right] + 1}$$

$$H(z) = \frac{a - az^{-2}}{(a+b+1) + (2-2b)z^{-1} + (b-a+1)z^{-2}}$$

$$H(z) = \frac{\alpha_0(1-z^{-2})}{1 + \alpha_1 z^{-1} + \alpha_2 z^{-2}}$$

Substitutions:

$$s = \frac{2}{T}\left[\frac{1-z^{-1}}{1+z^{-1}}\right]$$

$$a = 2\frac{RC}{T}$$

$$b = \left(\frac{2}{T}\right)^2 LC$$

$$\alpha_0 = \frac{a}{(a+b+1)}$$

$$\alpha_1 = \frac{(2-2b)}{(a+b+1)}$$

$$\alpha_2 = \frac{(b-a+1)}{(a+b+1)}$$

Final difference equation: $y[n] = \alpha_0 x[n] - \alpha_0 x[n-2] - \alpha_1 y[n-1] - \alpha_2 y[n-2]$

Digital Emulation of Analogue Networks III: Real-Time Performance

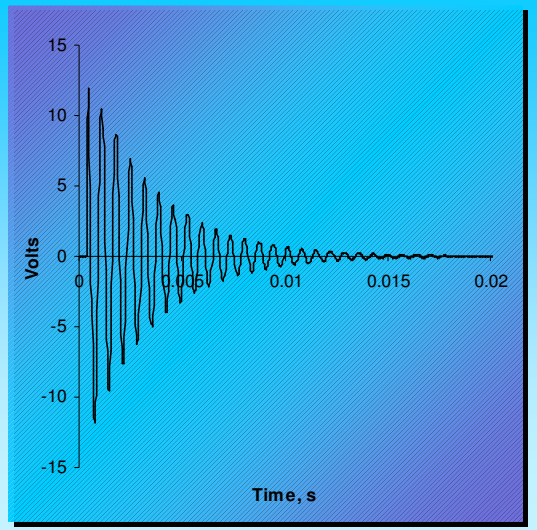

Design

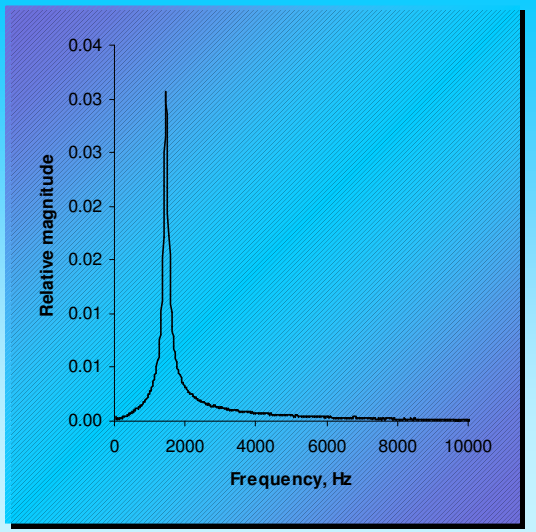

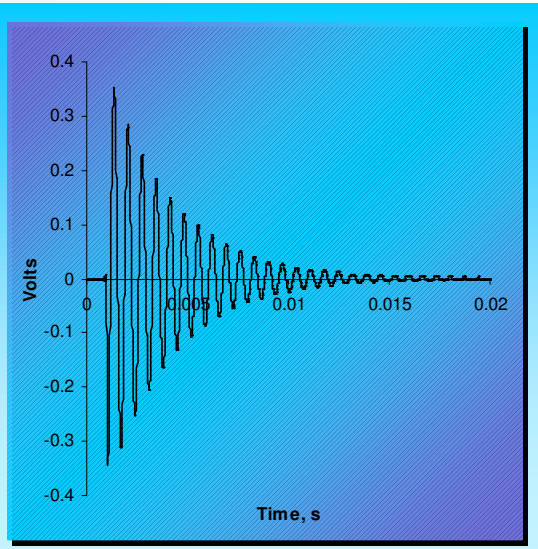

Realised

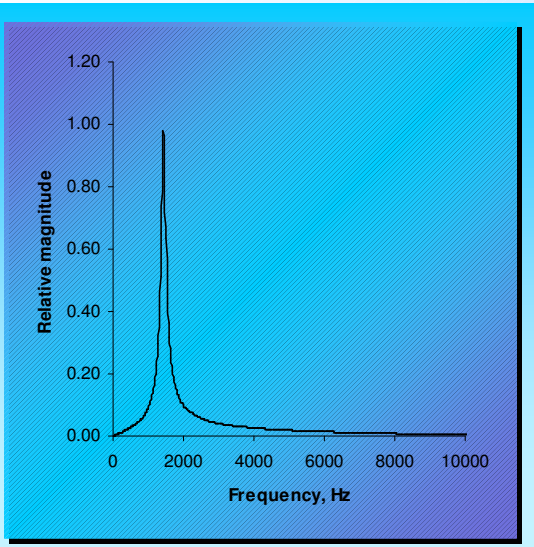

IIR Comb Filters and Pole-Zero Placement

$$H(z)=\prod_{k=0}^{n-1}\frac{z-z_k}{z-p_k}=\frac{(z-z_0)(z-z_1)}{(z-p_0)(z-p_1)}\times\frac{(z-z_2)(z-z_3)}{(z-p_2)(z-p_3)}\ldots\times\ldots\frac{(z-z_{n-2})(z-z_{n-1})}{(z-p_{n-2})(z-p_{n-1})}$$

$$H(z)=\frac{(z-z_0)(z-z_1)}{(z-p_0)(z-p_1)}$$

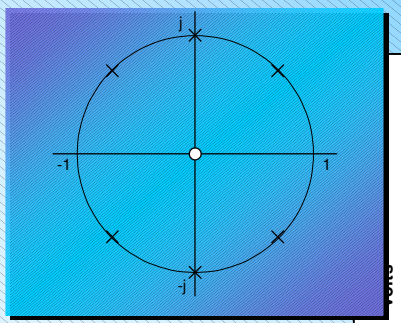

$$z_0=\alpha_0+j\beta_0$$
$$z_1=\alpha_0-j\beta_0$$
$$p_0=\alpha_1+j\beta_1$$
$$p_1=\alpha_1-j\beta_1$$

$$\varepsilon_0=\alpha_0^2+\beta_0^2$$
$$\varepsilon_1=\alpha_1^2+\beta_1^2$$

$$H(z)=\frac{[z-(\alpha_0+j\beta_0)][z-(\alpha_0-j\beta_0)]}{[z-(\alpha_1+j\beta_1)][z-(\alpha_1-j\beta_1)]}=\frac{1-2\alpha_0 z^{-1}+\varepsilon_0 z^{-2}}{1-2\alpha_1+\varepsilon_1 z^{-2}}$$

$$y[n]=x[n]-2\alpha_0 x[n-1]+\varepsilon_0 x[n-2]+2\alpha_1 y[n-1]-\varepsilon_1 y[n-2]$$

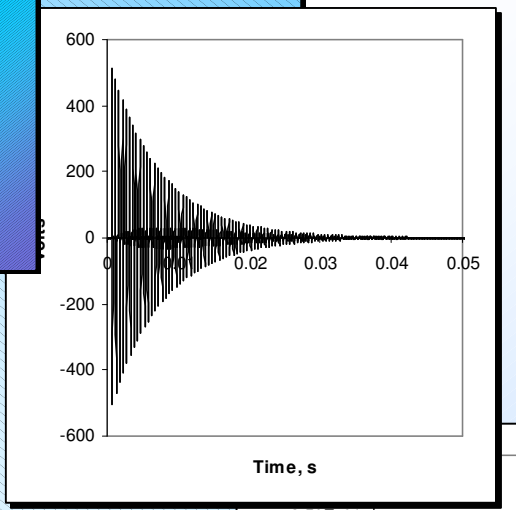

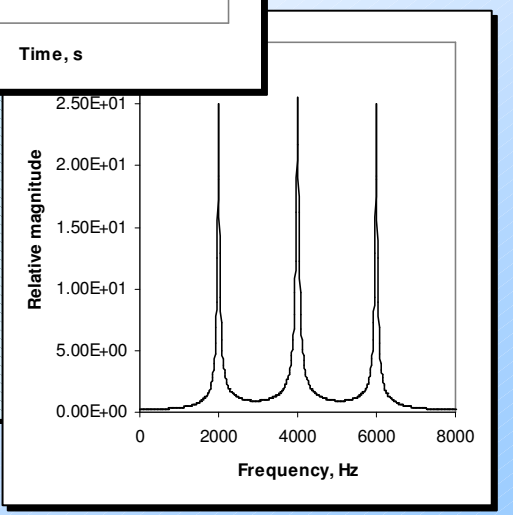

Inverse Filters: Design and Applications

$$y[n] = \sum_{k=0}^{M-1} \tilde{h}^{-1}[k]x[n-k]$$

Signal Shape Reconstruction

Essential Equations Describing Time Domain Deconvolution (Inverse Filtering) for Real-Time and Off-Line Processing

Simple Fourier domain scheme (rarely successful):

$$y(t) = x(t) * h(t) \Leftrightarrow Y(\omega) = X(\omega)H(\omega) \qquad x(t) = F^{-1}\left[\frac{Y(\omega)}{H(\omega)}\right]$$

Fourier domain scheme with noise estimate:

$$y(t) = x(t) * h(t) + s(t) \qquad x(t) = F^{-1}\left[\frac{Y(\omega)}{H(\omega)} - \frac{S(\omega)}{H(\omega)}\right]$$

Time domain scheme with noise estimate (surprisingly useful):

$$\tilde{h}^{-1}(t) = F^{-1}\left[\frac{1}{H(\omega) + s}\right] \qquad s = \begin{cases} 0, & if \quad \dfrac{1}{|H(\omega)|} < \gamma \\ 0 < s < 1, & otherwise \end{cases}$$

Finally:

$$x(t) = y(t) * \tilde{h}^{-1}(t)$$

Signal Shape Reconstruction in Practice

Signal comprising three impulses

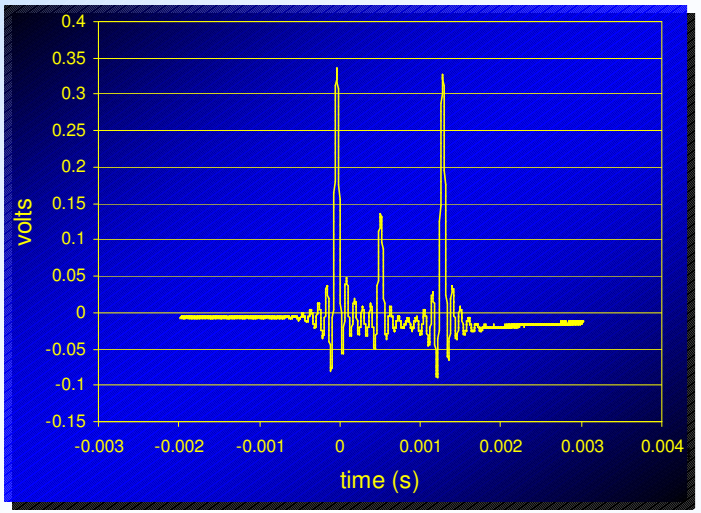

Signal after low-pass distortion

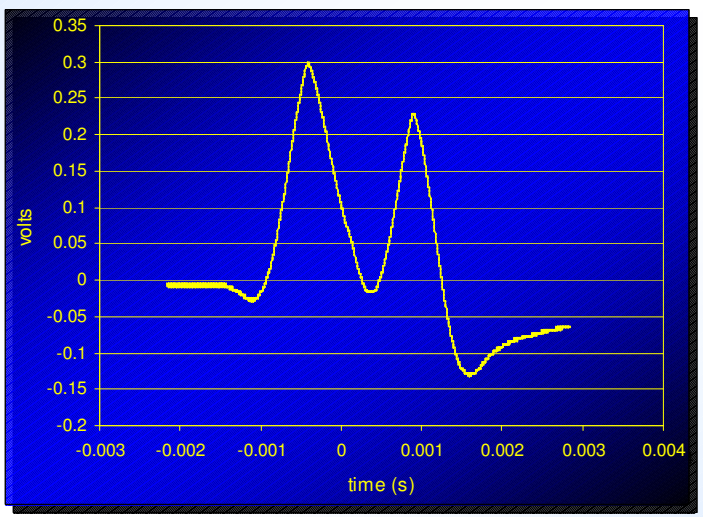

Signal after inverse filtering in real-time

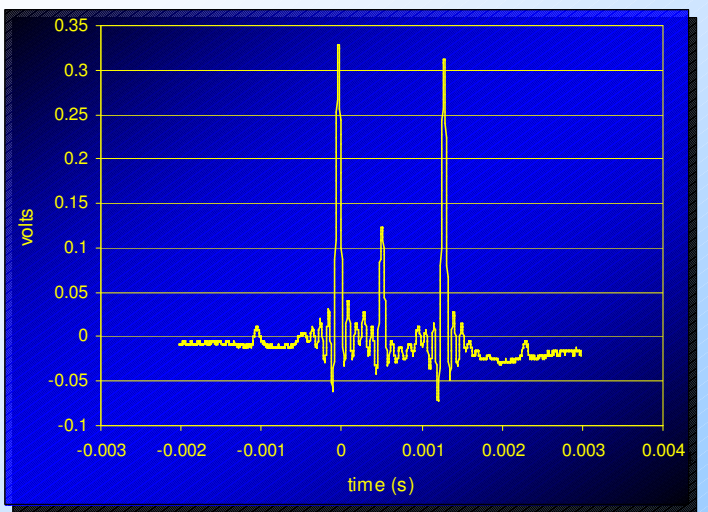

Case study 1: Detection of AC magnetic fields propagated through a ferrous steel boundary: The Skin Effect

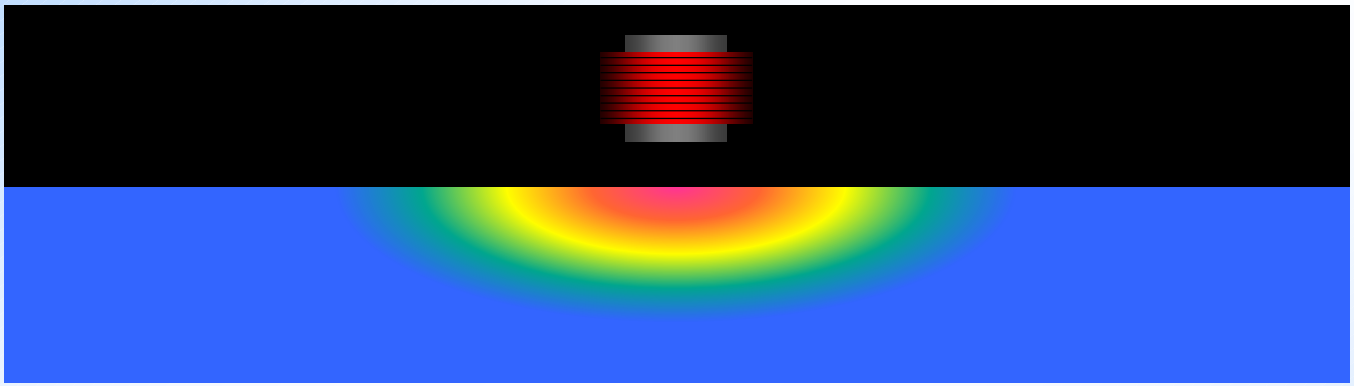

The strength of both the eddy currents and the associated magnetic field fall rapidly with depth in ferrous materials. The equation which describes the fall in current density is given by:

$$J = J_s e^{-\frac{d}{\delta}} . e^{j(\omega t - \frac{d}{\delta})}$$

Where J_s is the current density on the surface, d is the depth within the material, δ is the skin depth, ω is the angular frequency and J is the is the current density at depth d. The skin depth for a given material is governed by the relationship:

$$\delta = \sqrt{\frac{2}{\omega \mu_0 \mu_r \sigma}}$$

where σ is the conductivity of the conductor or target, μ_r its relative permeability and μ_0 is the absolute permeability of a vacuum.

Experimental Configuration

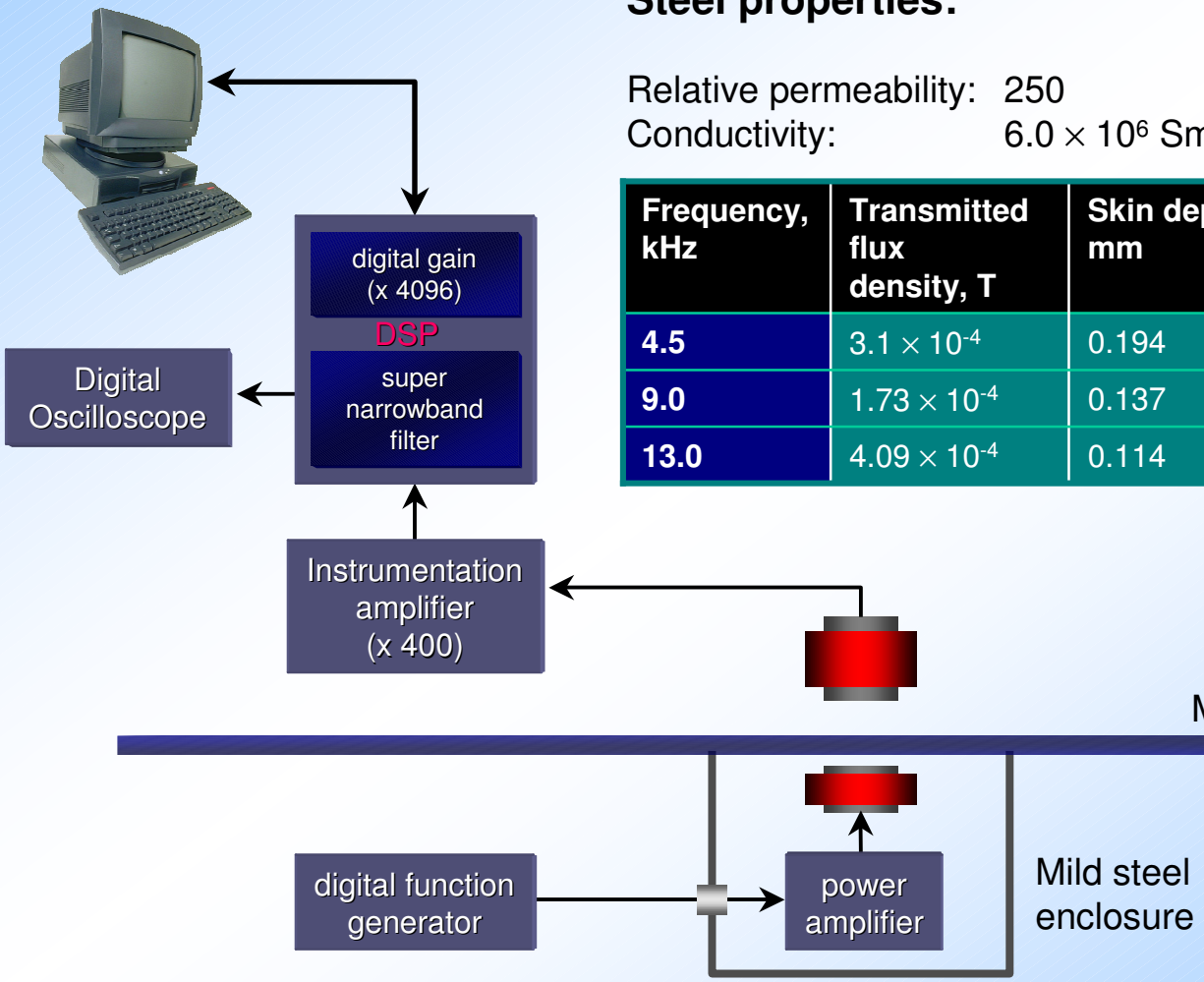

Steel properties:

Relative permeability: 250
Conductivity: 6.0×10^{6} Sm^{-1}

Frequency, kHz	Transmitted flux density, T	Skin depth, mm	Attenuation	Received flux density, T
4.5	3.1×10^{-4}	0.194	3.33×10^{-5}	1.03×10^{-8}
9.0	1.73×10^{-4}	0.137	4.57×10^{-7}	7.89×10^{-11}
13.0	4.09×10^{-4}	0.114	2.20×10^{-8}	8.99×10^{-12}

MANCHESTER 1824

The University of Manchester

Laboratory System

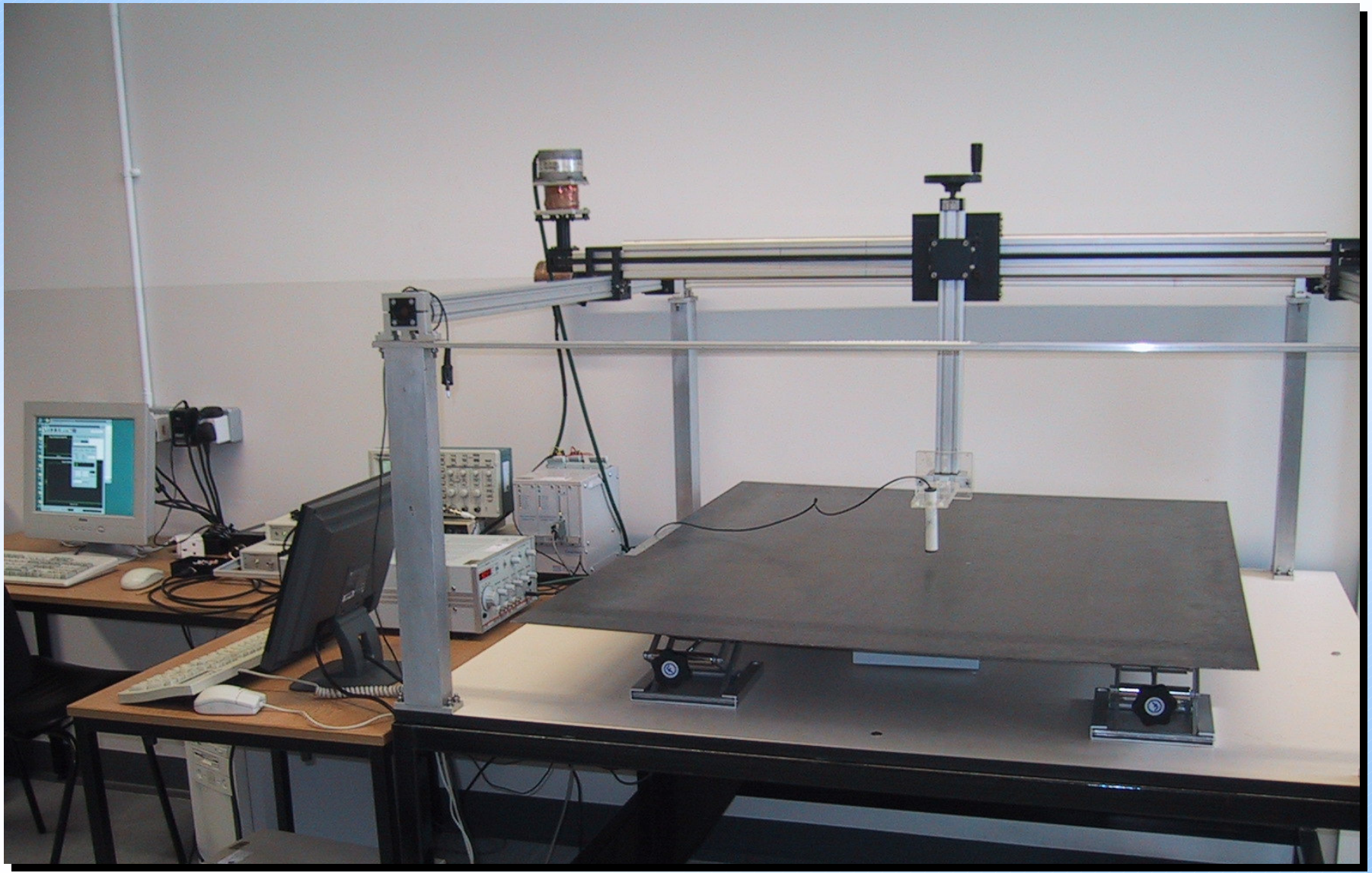

IIR Filter Frequency Response at 9 kHz

Pole locations for two IIR filters				
Centre Frequency, kHz	p_0, real	p_0, imaginary	p_1, real	p_1, imaginary
4.5	0.83146	0.55556	0.83146	-0.55556
9.0	0.38268	0.92387	0.38268	-0.92387

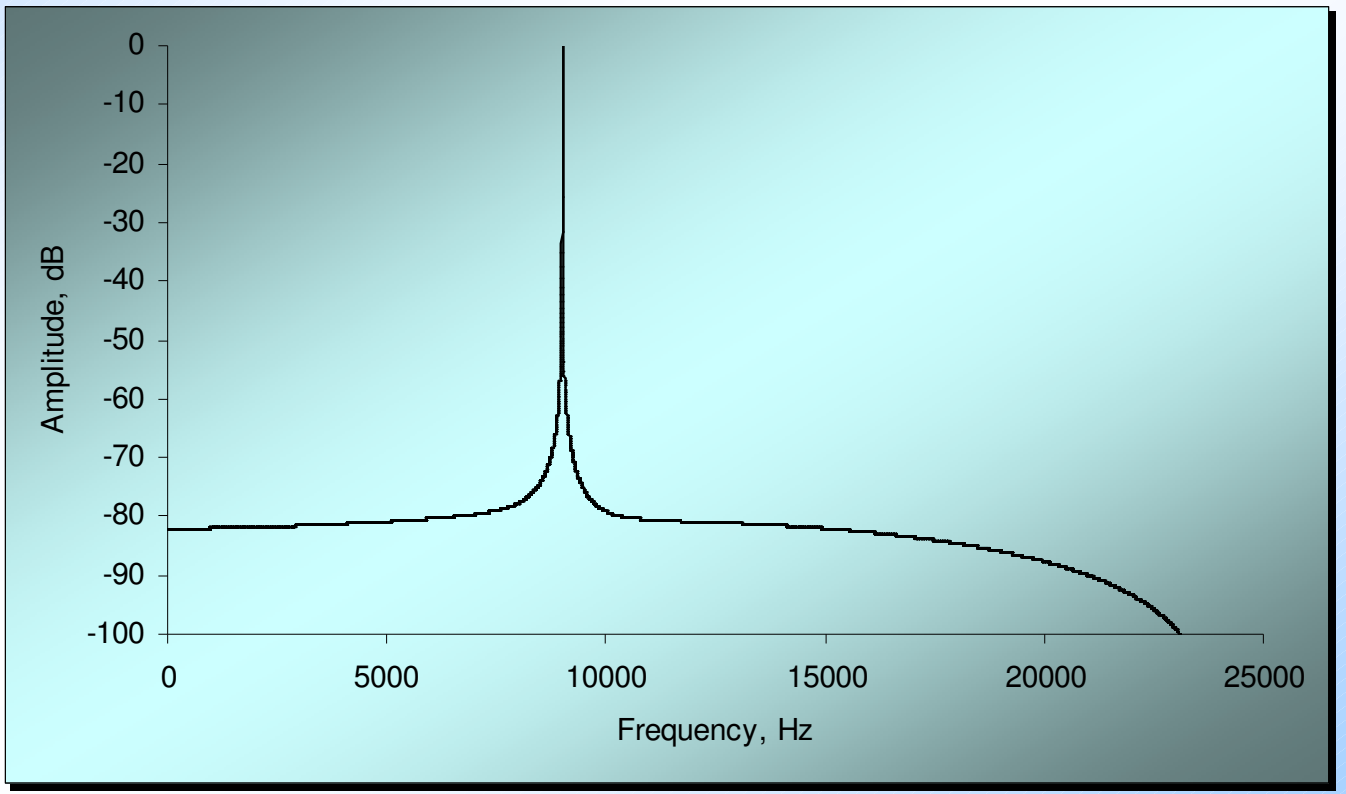

Line Scan Results at 4.5 kHz and 9 kHz

4.5 kHz

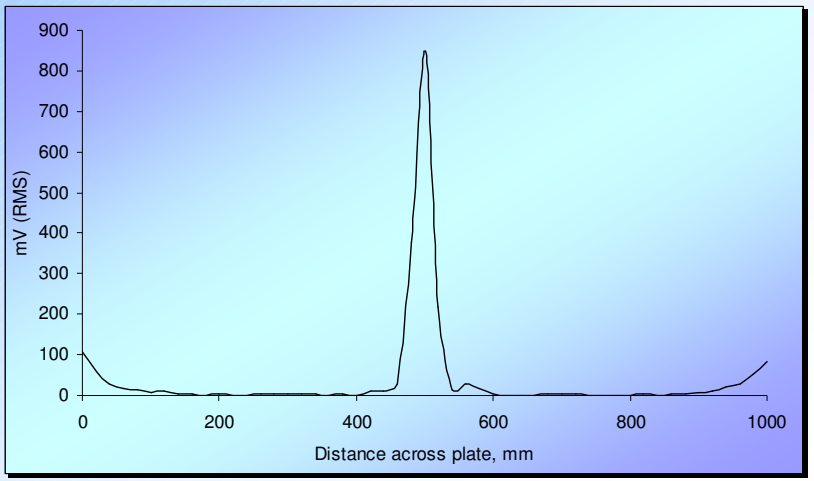

9 kHz

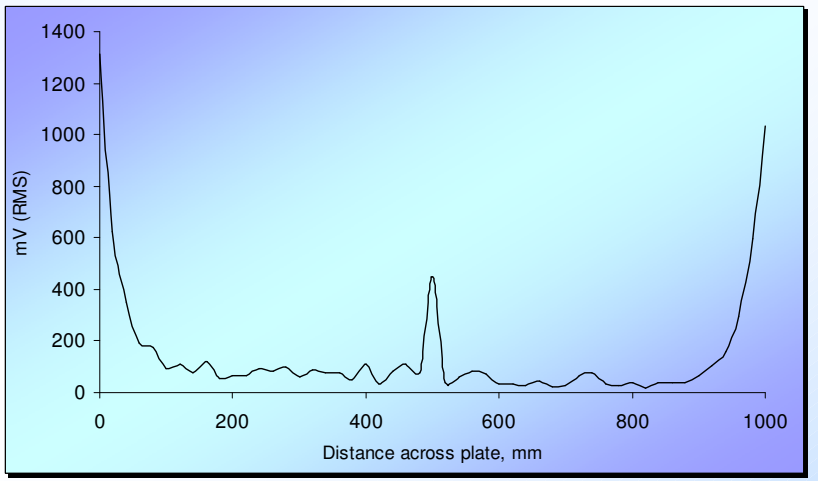

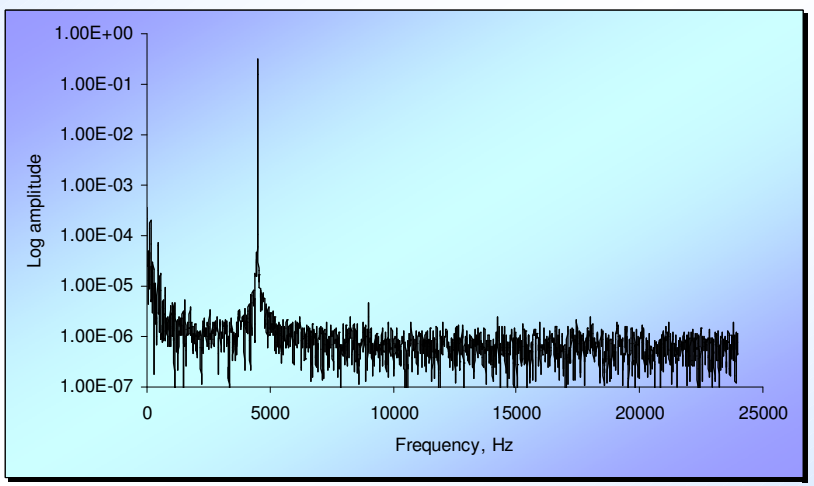

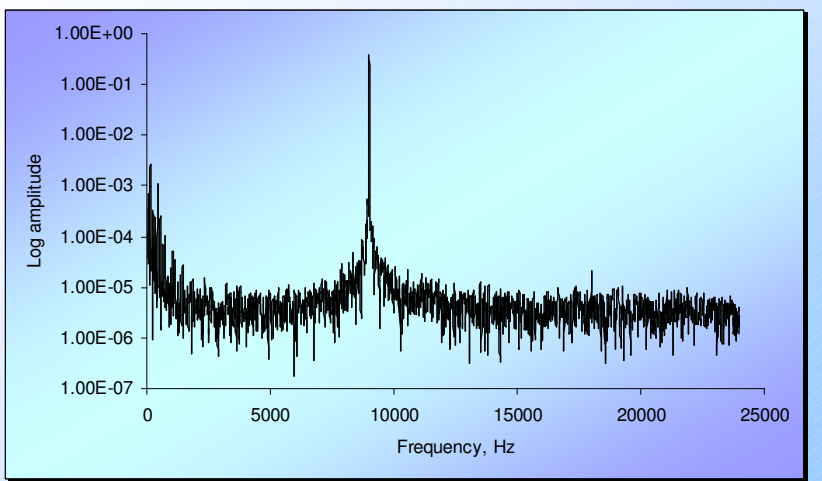

Case study 2: Detection of low amplitude ultrasonic pulses propagated through seawater via a steel structure

7 m structure being lowered into the dock at Liverpool, UK

Experimental Configuration

Signal type	Tone burst
Frequency	40 kHz
Transmission amplitude	20 V
Divergence angle	hemispherical
Attenuation	Geometric ($1/r^2$)
Peak received signal	650 nV

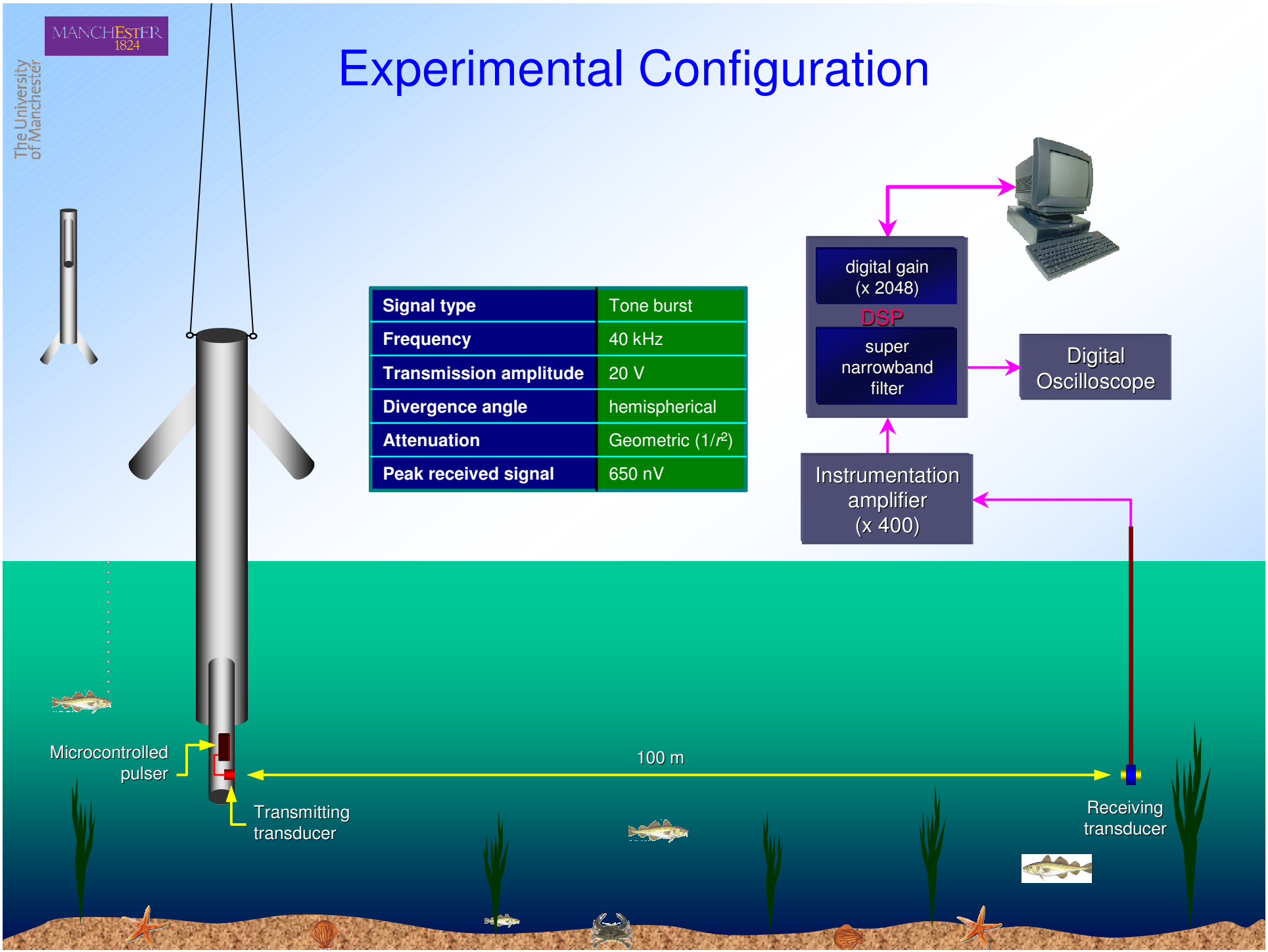

Typical Results

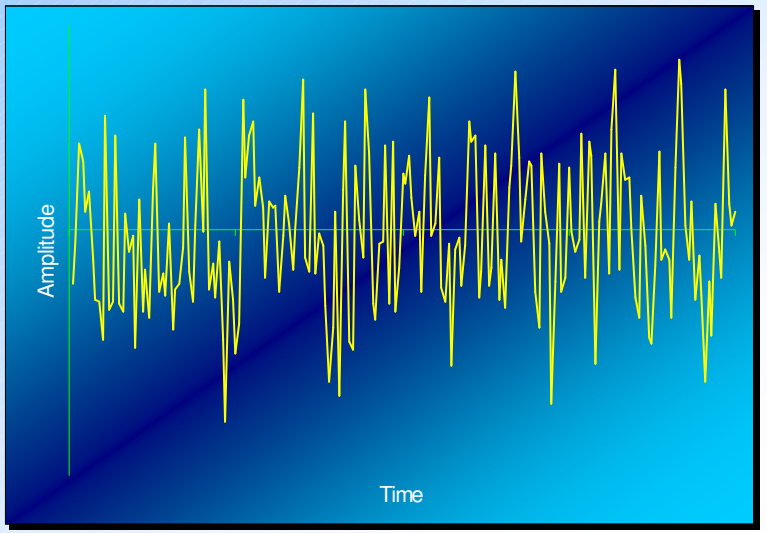

(a)

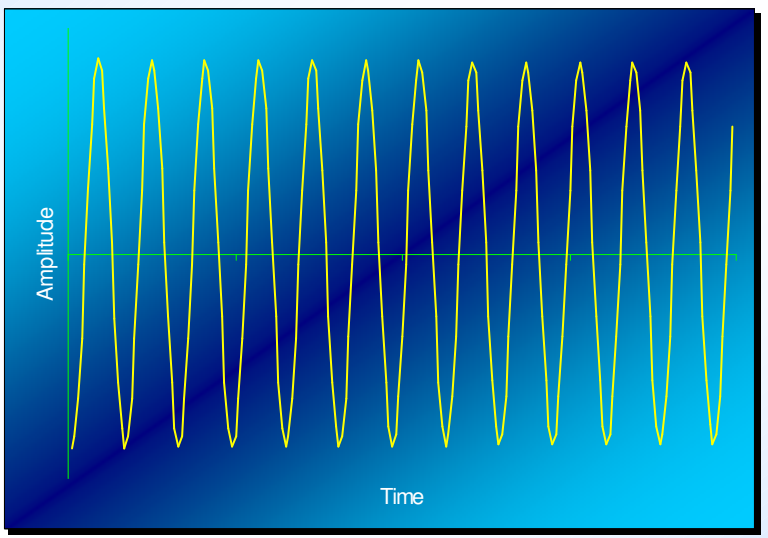

(b)

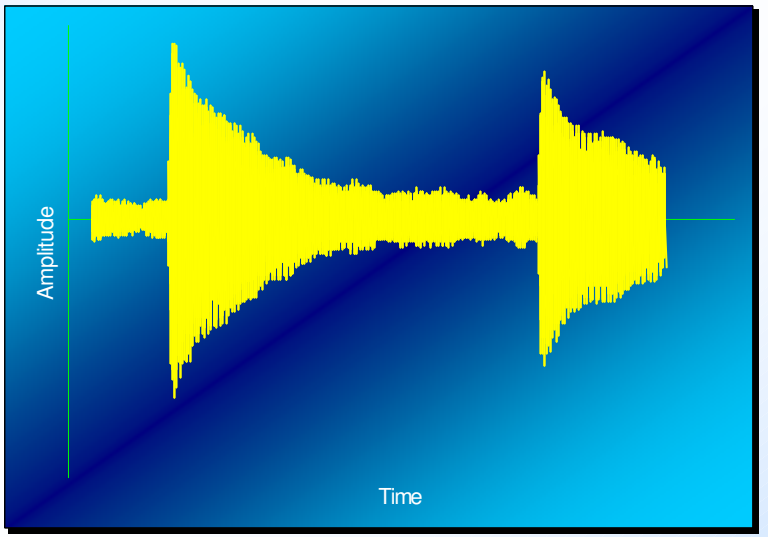

(c)

(a) Detail of original received signal degraded by noise.

(b) Detail of received signal, recovered by super narrowband filter.

(c) Complete tone burst signal detected after transmission through water, recovered using a super narrowband IIR filter.

Conclusions

- Flexibility ensures that real time DSP is suitable for many applications in weak field detection
- Software-realized processing yields very significant improvements with regard to stability, precision and repeatability
- Multiple frequencies can be interrogated simultaneously, unlike lock-in detection
- At least a factor of ten cheaper than lock-in detection
- New generation DSP devices are extending the range of signal frequencies over which real time discrete processing can be applied
- However: DSP system design requires investments in time and effort

MANCHESTER 1824

The University of Manchester

Acknowledgements

With thanks to Bosco Fernandes, Rito Mijarez, Graham Miller and Muhammad Zaid. We also acknowledge the EPSRC for financially supporting this work.